The Postglacial response of Arctic Ocean gas hydrates to climatic amelioration

Serov, Pavel; Vadakkepuliyambatta, Sunil; Mienert, Jürgen; Patton, Henry; Portnov, Alexey; Silyakova, Anna; Panieri, Giuliana; Carroll, JoLynn; Andreassen, Karin; Hubbard, Alun

Published in:
Proceedings of the National Academy of Sciences of the United States of America

DOI:
10.1073/pnas.1619288114

Publication date:
2017

Citation for published version (APA):
Serov, P., Vadakkepuliyambatta, S., Mienert, J., Patton, H., Portnov, A., Silyakova, A., Panieri, G., Carroll, J., Andreassen, K., & Hubbard, A. (2017). The Postglacial response of Arctic Ocean gas hydrates to climatic amelioration. *Proceedings of the National Academy of Sciences of the United States of America*, *114*(24), 6215-6220. https://doi.org/10.1073/pnas.1619288114

The post-glacial response of Arctic Ocean gas hydrates to climatic amelioration.

Pavel Serov[1], Sunil Vadakkepuliyambatta[1], Jürgen Mienert[1], Henry Patton[1], Alexey Portnov[1], Anna Silyakova[1], Giuliana Panieri[1], Michael Carroll[1,2], JoLynn Carroll[1,2], Karin Andreassen[1], Alun Hubbard[1]

[1]CAGE - Centre for Arctic Gas Hydrate, Environment and Climate, Departmnet of Geosciences, UiT - The Arctic University of Norway, Tromsø, Norway; [2]Akvaplan-niva, Tromsø, Norway

Submitted to Proceedings of the National Academy of Sciences of the United States of America

Seafloor methane release due to the thermal dissociation of gas hydrates is pervasive across the continental margins of the Arctic Ocean. Furthermore, there is increasing awareness that shallow hydrate-related methane seeps have appeared due to enhanced warming of Arctic Ocean bottom water during the last century. Whilst it has been argued that a gas hydrate gun could trigger abrupt climate change, the processes and rates of subsurface/atmospheric natural gas exchange remain uncertain. Here we investigate the dynamics between gas hydrate stability and environmental changes from the height of the last glaciation through to the present day. Using geophysical observations from offshore Svalbard to constrain a coupled ice sheet/gas hydrate model, we identify distinct phases of subglacial methane sequestration and subsequent release on ice sheet retreat that led to the formation of a suite of seafloor domes. Reconstructing the evolution of this dome field, we find that incursions of warm Atlantic bottom water forced rapid gas hydrate dissociation and enhanced methane emissions during the penultimate Heinrich event (H1), the Bølling and Allerød interstadials and the Holocene optimum. Our results highlight the complex interplay between the cryosphere, geosphere and atmosphere over the last 30,000 years that led to extensive changes in sub-seafloor carbon storage that forced distinct episodes of methane release due to natural climate variability well before recent anthropogenic warming.

gas hydrate | Arctic Ocean | methane release | climate change

Introduction

Marine surveys of the Arctic Ocean continental shelf and slope are continuously disclosing new seafloor methane seeps associated gas hydrate reservoirs[1-3]. Gas hydrates are crystalline solids that consist of methane trapped in a lattice of hydrogen-bonded molecules of water[4]. Due to their extensive distribution throughout the Arctic and elsewhere, hydrates are an integral part of a dynamic global carbon cycle[5,6] where methane and heavier gases (i.e. ethane/propane) are sequestered and released over time. Under stable - high pressure/low temperature conditions - gas hydrates constitute a potentially massive natural sub-seafloor carbon sink and storage capacitor. Yet even under stable conditions, some ongoing methane seepage is likely to occur due to preferential fluid migration from deep, thermogenic hydrocarbon reservoirs or due to methanogenesis within organic-rich marine sediments. Despite this, under warming and/or de-pressurization, hydrate dissociation can drive large-scale natural gas release with potentially profound impacts. Abrupt episodes of methane emissions from the seafloor may attain the atmosphere[6] and thereby become a potent feedback for abrupt climate change[5,7]. Methane released into the water column also affects its geochemical signature and pH due to aerobic oxidation leading to enhanced levels of carbon dioxide[8]. Yet, moderate methane release is regulated by, and is also the basis for marine chemosynthetic ecosystems that thrive in the vicinity of venting gas seeps, with new extremophiles continually discovered[9-11]. Gas hydrates also sculpt and influence seafloor morphology with methane-derived carbonate crusts and pavements formed above gas venting systems and, furthermore, hydrate dissociation within sediments has been linked to mega-scale submarine landslides[12], pockmarks[13], craters[14] and gas dome structures[15].

Gas and water that constitute a hydrate crystalline solid within the pore space of sediment remains stable within a gas hydrate stability zone (GHSZ) that is a function of bottom water temperature, sub-bottom geothermal gradient, hydrostatic and lithostatic pressure, pore water salinity, and the specific composition of the natural gas concerned. Generally, the GHSZ increases in thickness with greater water depth[4]. In contrast to other Arctic regions, where gas hydrates remain stable to 300 meters below sea level (mbsl), or even shallower in subsea permafrost regions[16], the modern GHSZ along the south-western Svalbard margin appears deeper at 370 - 390 mbsl. Here, the relatively warm, $\sim$2.7 ^{o}C northward flowing West Spitsbergen Current exerts strong control on the spatial extent and thickness of the GHSZ. It has been argued that recent warming of this current has triggered active recession of the upper GHSZ thereby promoting enhanced methane seepage[17,18]. An alternative hypothesis suggests that seasonal variations in bottom water temperature drive fluctuations of gas hydrate decomposition and transient methane release[19]. To date, gas hydrates have not been observed at or close to the upper edge of hydrate stability zone offshore of Svalbard. Due to the largely unknown composition of gas in marine sediments coupled with a paucity of cores and actual hydrate samples, previous estimates for the GHSZ[17,19] are based on theoretical considerations alone which may to be at odds with the actual hydrate stability conditions at the seabed. Thus, the fate of gas hydrates on the Svalbard margin in response to past, ongoing and future oceanic warming remains unclear.

Here, we present the new discovery of intensive cold seep activity clustered on the apexes of several $\sim$500 m wide gas hydrate-bearing domes at 370-390 mbsl in Storfjordrenna, northwestern Barents Sea (Figure 1). Such formations, close to the shallow termination of the GHSZ, have rarely been observed

Significance

Shallow Arctic Ocean gas hydrate reservoirs experienced distinct episodes of subglacial growth and subsequent dissociation that modulated methane release over millennial timescales.

Reserved for Publication Footnotes

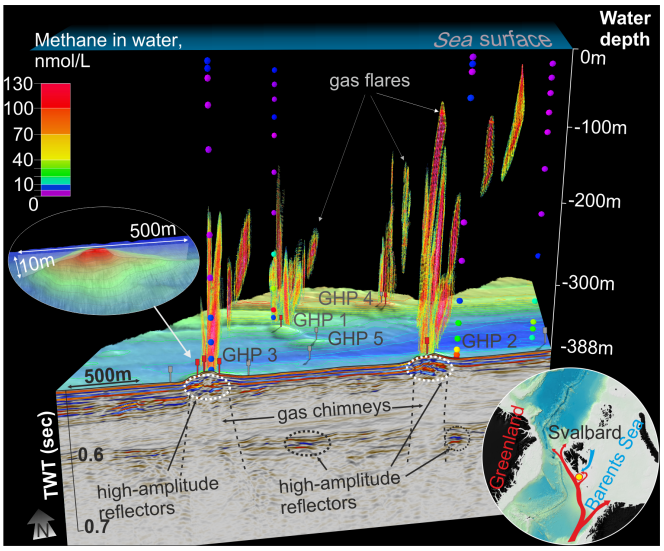

Fig. 1. - Gas leakage system at Storfjordrenna. Compilation of observations, including seabed topography from high-resolution multibeam data (10 m grid cell), 2D seismic cross-section (300 Hz) and single beam echosounder data (38 kHz) tracing streams of gas bubbles (gas flares) in the water column. Different colors within gas flares indicate backscattering strength of the reflected acoustic signals (red is the highest values, light green is the lowest). Vertical trains of large dots in the water column show locations of the water samples and, by colors, - concentrations of dissolved methane measured. Red and grey marks at the seafloor indicate coring sites with and without gas hydrates, respectively. On the insert red arrow shows West Spitsbergen Current (warm Atlantic Water), blue arrow – East Spitsbergen Current (cold Polar Water).

in the Arctic and their origin has yet to be investigated. We refer to these domes as "gas hydrate pingos" (GHPs) since they are morphologically similar to ice-bearing onshore pingos[20] and their offshore counterparts[21,22]. Terrestrial and offshore pingos form in permafrost regions where water-saturated soils freeze and expand[20,23]. The primary difference between the permafrost-related mounds and the domes imaged here is that instead of ice, GHPs are formed from methane-derived authigenic carbonates and gas hydrates, which render them susceptible to changes in their ambient temperature and pressure environment.

The wider Barents Sea region experienced profound subglacial temperature, pressure and isostatic variations during the last glacial cycle[24-26]. A cooling climate ~35,000 years ago initiated the growth of the marine-based Barents-Kara Sea ice sheet providing extensive high pressure/low temperature subglacial conditions across the continental shelf off Svalbard[13]. Analysis of sediment cores from the region reveal that the ice-sheet advanced across the shelf at ~27,000 cal. a BP and was at its maximum extent at the shelf break west of Svalbard by ~24,000 cal. a BP[27]. After a prolonged period of relative stability, deglaciation commenced rapidly from ~20,000 cal. a BP[28,29] onwards. Hemipelagic muds present in a sediment core from Storfjordenna, some 12 km south of our GHP site, constrains local deglaciation to around 19,000 cal. a BP[30]. The receding ice sheet left a series of grounding zone wedges and several generations of plough-marks indicating alternating phases of standstill and active, calving retreat[29]. Concurrent with and promoting deglaciation, ambient Arctic water of ~1.5°C, encroached onto the shelf[30]. Marine sediment $\delta^{18}O$ records reveal that during the Heinrich event 1 (15,000 -13,000 cal. a BP), Bølling and Allerød interstadials (13,000 – 11,000 cal. a. BP), and the Holocene Optimum (9,000 – 8,000 cal. a BP), Atlantic bottom water - on average 3°C warmer - displaced the cooler ambient Arctic water body that was present immediately after deglaciation[30,31].

Storfjordrenna's complex environmental history and that of the wider Barents Sea shelf, raises several important questions in relation to gas hydrate storage and decomposition. Did the GHPs develop as a result of deglaciation or due to more recent ocean warming? How did the GHSZ respond to ice sheet retreat and the subsequent marine incursion of Arctic waters? When and for how long did stable gas hydrates exist during glaciation? How thick were they? Addressing these questions requires a quantitative and unified understanding of the interaction between the ice sheet, ocean and subsurface methane hydrate reservoir over timescales spanning the last glaciation into the near future. To this end, we characterise the newly discovered site at Storfjordrenna, along with the first documented recovery of gas hydrate from the Svalbard-Barents Sea shelf, to provide boundary conditions for a time-dependent coupled ice sheet/GHSZ model that describes the evolution and dynamics of the glacial and subglacial gas hydrate systems in this sector.

Gas hydrate pingos and methane venting

Five discrete GHPs were geophysically imaged within a 2.5 km^2 area on the flank of the glacially eroded cross-shelf Storfjordrenna (Figures 1 and supplementary Figure S1). All the GHPs have sub-circular or elongated shapes with diameters of 280-450 m and heights of 8-10 m. Their existence within a ground-zone of vigorous paleo-ice stream activity evidenced by multiple mega-scale glacial lineations indicates formation after the last ice sheet retreated from the area.

Hydro-acoustic observations reveal that four out of five GHPs persistently emit natural gas (Figure 1). Gas bubbles, represented by hydroacoustic anomalies within the water column, emerge and concentrate from the topographic summits of the GHPs. The area was surveyed three times in May, July and October 2015 and the observed gas flares were continuous, with many of them rising to at least ~200 mbsl and the largest ones rising to 20 mbsl. Undetected bubbles – those smaller than the resonance frequency of the echosounder signal (~0.6 and 0.8 mm at 20 and 200 m water depth, respectively) cannot be discounted from breaking the ocean surface without being traced[32]. Despite the lower hydrostatic pressure, rising methane bubbles gradually shrink by diffusion into the ambient water column[33,34]. Geochemical analysis indicates that gas seepage supplies the water column with up to 130 ml/l of dissolved methane (Figure 1), some ~40 times higher than the ambient concentration. A towed camera vehicle equipped with a methane sensor surveyed 0.5 to 2.0 m above seabed and traced concentrated plumes of dissolved methane associated with the GHPs. The location of the methane plumes along with the gas release sites coincide with the GHP summits, confirming that persistent, focused methane expulsion is closely linked to the specific morphology of each GHP (Figure 1).

Cores acquired from the GHPs reveal that gas hydrate-bearing hemipelagic sediments with abundant carbonate concretions (supplementary figure S2) are present in distinct layers below the seafloor (40-70 and 90-120 cm below the seafloor in GHP's summits; 120-130 and 205-220 cm below seafloor in the GHPs' flanks). Outside the GHPs, sediments do not contain carbonate inclusions indicating reduced or absent influx of methane. In a pattern identical to gas expulsion and flares, gas hydrates appear exclusively within the topographic highs comprising multiple layers with different textures that include disseminated, massive and layered hydrates that occur at various depths within the cores. Some sediment layers exhibit a liquefied, soupy material due to the dissociation of hydrates that is typically observed in recovered sediment cores where the temperature and pressure conditions have changed greatly on opening[35,36]. For all GHPs cores, the released gas was predominantly methane with an unambiguous thermogenic (i.e. depleted) isotopic signature ($\delta 13C_{average}$ =-47,

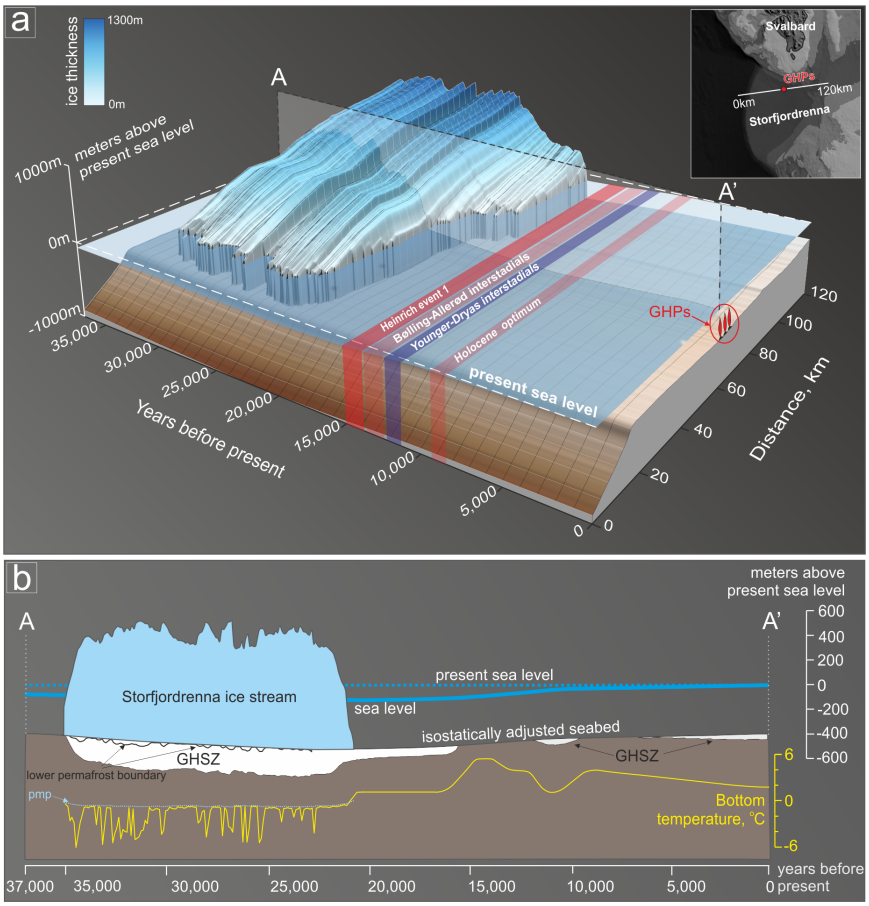

Fig. 2. - Evolution of the Storfjordrenna ice stream and postglacial oceanographic changes. a – time-lapse setting of the ice stream along the line indicated in the insert. GHPs are not to vertical and horizontal scale. b – Changes of the ice and GHSZ thickness, bottom temperature, sea level[59] and isostatically adjusted seabed at GHP site throughout the last 37,000 years.

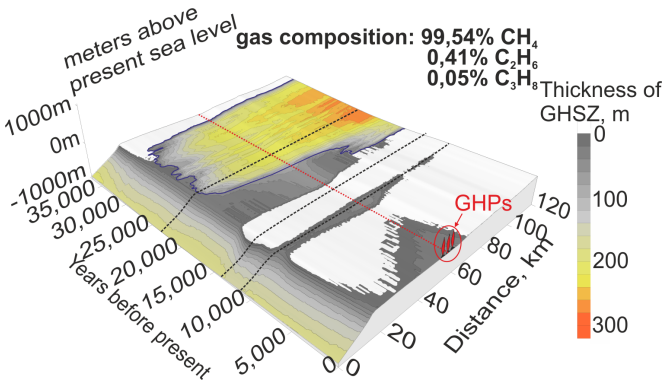

Fig. 3. - Evolution of GHSZ in outer Storfjordrenna throughout the last glacial cycle. Blue line indicates contours of the ice sheet. Red dashed line shows location of GHP site. GHPs are not to vertical and horizontal scale.

n=8; $\delta D_{average}$=-177; n=8) with additional low admixtures of higher methane homologs (C1/C2-$C3_{average}$ = 111.3; n=87) (table 1 supplementary).

High-resolution seismic data reveal deep-rooted (>150 m below seafloor) sub-vertical amplitude masking zones underlying each of the GHPs that we interpret as chimneys through which thermogenic-derived gas migrates upward (Figure 1). High-amplitude reflectors around these gas chimneys indicate local accumulations of free gas, gas hydrate or authigenic carbonates. Given these seismic data and the regional geological setting, we infer that an existing fault system within the upper Paleocene-Eocene and Pliocene-Pleistocene sedimentary rocks provide high permeability zones for upward thermogenic gas migration from underlying hydrocarbon rich Triassic-Jurassic formations[37-39].

Glacial history and evolution of gas hydrate stability

During the Last Glacial Maximum, a large grounded ice stream occupied Storfjordrenna and drained ice from a major accumulation centre over southern Svalbard[40]. Empirically constrained ice flow modelling reveals that grounded ice entered Storfjordrenna ~35,500 years ago with the onset of glaciation, overriding todays GHP site[25]. Within the next 2,000 years (by ~33,500 years ago), the Storfjordrenna ice stream had advanced to the shelf break (Figure 2a). During the next ~10,000 years, the ice stream was relatively stable, experiencing only minor fluctuations of the ice front, which was mostly pinned to the continental shelf edge. Ice was between 900 to 1000 m thick above the GHP site at this time, while subglacial temperatures fluctuated between -0.5 °C (the pressure-dependent melting point of ice) and -6°C dependent on the ice stream configuration (Figure 2b). Ice-sheet retreat commenced around 22,500 years ago in line with global climate amelioration. The active ice stream retreated from the GHP site ~21,000 years ago until it attained a stable position 40 km further upstream around 18,000 years ago. Under continued atmospheric and ocean warming coupled with ongoing eustatic sea-level rise, the ice stream retreated back to inner Storfjorden by 14,500 years ago.

By coupling the glacial evolution with a transient gas hydrate model (see Methods), we underscore the tight spatial and temporal relationship between GHSZ depth in Storfjordrenna and ice sheet dynamics (Figure 3, Figure 4). The GHSZ model essentially solves the conductive heat flux equations based on ambient pressure and thermal conditions provided by ice and/or

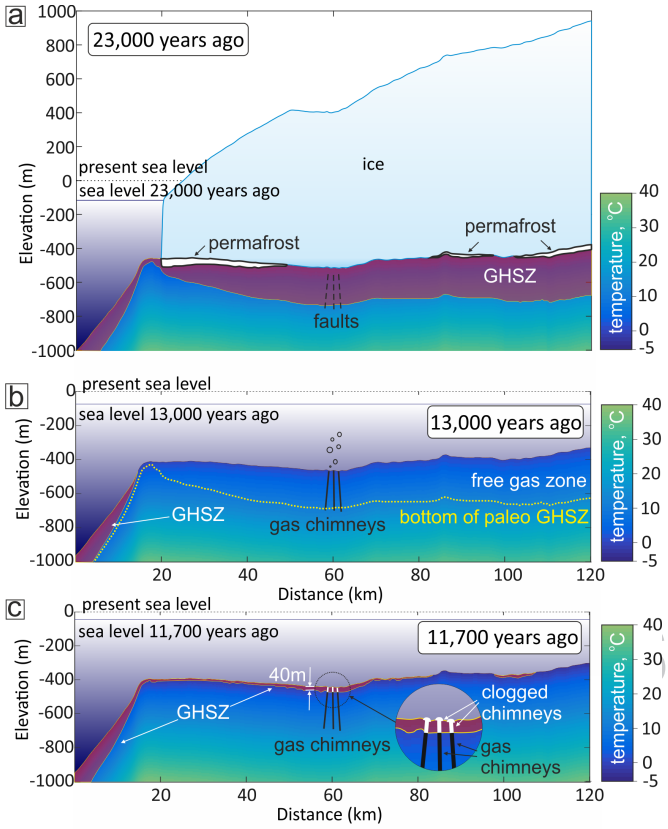

Fig. 4. - Growth and collapse of GHSZ in outer Storfjordrenna. Isostatic movements, subsurface temperature distribution, GHSZ, thickness of ice and permafrost resulted from our modelling. Gas chimneys and faults are not to vertical and horizontal scale. a – setting during the last glacial maximum: ~200 m thick GHSZ, patches of subglacial permafrost. b – GHSZ-free shelf during the Heinrich event 1. Seabed gas efflux is unhampered. c – continuous GHSZ on the shelf by the end of the Younger Dryas Interstadial. Gas chimneys intersect with ~40m GHSZ.

ocean above and geothermal inputs from below. A more sophisticated multiphase fluid flow model could be adopted but robust application of such a model requires accurate definition of a wide range of input parameters related to sediment and fluid properties, along with their evolution over time. Given the complex geological and environmental history at our study site, including significant episodes of glacial erosion/isostasy, compaction of sediments, subglacial and marine deposition, formation and melting of subglacial permafrost – all of these conditions would require accurate parameterization in a multiphase model. Hence, given the available data and the environmental complexity of the study site, we reason that application of a GHSZ model is a more pragmatic and robust approach in this instance.

The GHP site and adjacent shelf were outside of the GHSZ until the onset of ice sheet advance 35,000 years ago (Figure 2b, Figure 3). Cold subglacial temperatures (-2°C_{mean}) combined with high overburden pressures in excess of 8 MPa (equating to 900 m overburden ice), established a ~200 m thick subglacial GHSZ at the GHP site that sustained for 13,500 years. Around 30,000 years ago the subglacial GHSZ merged with the subseafloor GHSZ on the continental slope, forming a continuous gas hydrate field across the entire region (Figure 3). Throughout this glacial episode, the thickness of the subglacial GHSZ varied by around 20%, dependent on ice thickness, basal temperatures and concomitant overburden pressure (Figure 2b). After final deglaciation, the impact of an inherited glacio-isostatic depression of ~85 m at the GHP site promoted the preservation of a 100 m thick GHSZ up until around 15,500 years ago (Figure 2b, Figure 3). Eventually though, inflowing warm Atlantic Water at 4.0 to 5.5 °C associated with the Heinrich 1 (H1) event and the Bølling-Allerød interstadials[30] combined with ongoing isostatic rebound destabilised any remnants of the GHSZ from the area (Figure 3). Northern Hemisphere cooling during the Younger Dryas stadial at ~12,000 years ago and the incursion of the cold East Spitsbergen Current[30] initiated a second phase of gas hydrate formation with a ~60 m thick GHSZ established across the shelf that once again connected with the persistent offshore GHSZ beneath the continental slope (Figure 3).

Analogous to H1, the Holocene optimum was likewise associated with an intrusion of warm, ~4 °C Atlantic Water from outer Storfjordrenna, and led to a further episode of gas hydrate destabilisation (Figure 3). From 8,000 years onwards a steady transition to modern oceanographic conditions - with bottom water temperatures experiencing a steady decline from 4.0 to 2.0°C – somewhat surprisingly promoted moderate gas hydrate growth at the GHP site up to the present. Today, Storfjordrenna hosts two competing water masses: warm and saline Atlantic Water and Arctic Water that is cold and fresh, the interplay of which yields strong seasonal fluctuations in bottom water temperature from 0.5 to 2.0 °C dependent on prevailing synoptic conditions[41]. Annual bottom water temperatures observed since the 1950s[42] have though remained steady and thus gas hydrates in the area have remained stable (assuming a similar gas composition to that at the GHP site - supplementary Figure S3).

Varying methane leakage activity

Through synthesis of direct observations with hybrid ice sheet/GHSZ modelling, we demonstrate that an extensive, well-developed subglacial gas hydrate system formed across outer Storfjordrenna during the Last Glacial Maximum. This hydrate system subsequently experienced repeated cycles of re-emergence/dissociation during the Late Glacial and Holocene periods driven by changes in oceanographic conditions and gradual glacio-isostatic recovery. Due to its episodic nature, the changes in the GHSZ forced distinct phases of seafloor methane expulsion. During phases when the seafloor was within the hydrate stability envelope, gas hydrate growth incorporated existing natural gas, partially filling sediment pore space and thereby reducing its permeability to ascending fluid flow. Conversely, during phases of gas hydrates decomposition, seafloor gas emissions were amplified due to hydrate-bound gas release and free gas venting from deeper thermogenic reservoirs.

The occurrence of discrete layers of methane-derived authigenic carbonates in shallow sediment cores acquired from the GHPs support our inference of distinct phases of enhanced methane release since deglaciation. Increased methane flux induces anaerobic oxidation of methane near the seafloor, which produces excess HCO^{3-} thereby enhancing authigenic carbonate precipitation [43,44]. Hence, high methane seepage activity associated with conditions of hydrate dissociation are favorable for carbonate precipitation.

The Barents Sea ice sheet covered the West Svalbard shelf for over 13,500 years, driving continuous gas entrapment in and beneath a thick and extensive subglacial GHSZ. On regional deglaciation, the corresponding abrupt increase in temperature and decreased pressure conditions triggered a period of thinning and shrinkage of the GHSZ (Figure 2b, 3). Reduced pressure and warmer bottom waters resulted in the complete disappearance of GHSZ within <5,000 years after the ice sheet retreated from shallow regions of the seafloor. Throughout the post-glacial period, a ~5 m thick section of hemipelagic sediments containing present gas hydrates and authigenic carbonates were deposited across the seafloor[28,30]. Driven by the pronounced warming of

bottom water to 5.5 °C[30] from 15,500 years ago onwards, any remnant GHSZ collapsed thereby releasing gas hydrates that had accumulated for more than 18,000 years. Decomposition of gas hydrates caused pore volume expansion and activated large scale release of formerly hydrate-bound methane that was vented through gas chimneys in the seafloor. Laboratory experiments and numerical simulations of seabed gas dome growth indicate that buoyancy forces and the corresponding enhanced pressure from upwelling methane confined within a gas chimney is sufficient to create seabed domes of a few hundred meters in diameter[45-47]. We propose that it was this excess pressure-related doming that initiated the growth of the GHPs around 15,500 years ago.

Corresponding to the Younger Dryas, a ~1,000 year episode of oceanic cooling stimulated extensive GHSZ regrowth and the cessation of methane seepage across the shelf (Figure 3, Figure 4c). Gas hydrate heaving, a process analogous to frost heave under permafrost conditions, also would have contributed to sediment upheaval within GHPs at this time. Successive fracturing of sediments caused by excess pore pressure would have led to cracks that eventually fill with hydrates[48], thereby leading to further GHP volume expansion.

A rapid recession of the GHSZ took place associated with a warming period of bottom water at the Holocene Optimum (Figure 3). From ~6,500 years ago onwards, oceanographic conditions were broadly comparable to those today, with Arctic-derived bottom waters (<2 °C) prevailing in outer Storfjordenna. These cooler oceanic conditions gradually led to the establishment of a new GHSZ up to 60 m thick that has persisted through to the present day (Figure 3). Our analysis demonstrates that complex changes in temperature and pressure conditions led to episodic gas hydrate formation in outer Storfjordrenna, which strongly modulated seafloor methane release, the formation of authigenic carbonates and GHPs during the Late Pleistocene and Holocene.

Besides Storfjordeanna, several glacial troughs with depths in excess of 350 mbsl have been eroded into the Barents and Kara Sea shelf (Figure 4a). These troughs and associated deeper shelf areas must have developed extensive GHSZ during the last glaciation which subsequently experienced episodic phases of collapse and re-emergence driven by changing subglacial, isostatic and oceanographic conditions[49-51]. Given the abundance of hydrocarbon provinces within these formerly glaciated margins, we propose that the GHPs we document here could be more common and extensive across the Arctic where submarine gas hydrate systems exist. Recent surveys off West Greenland support this proposition, where hydrate-bearing seafloor features appear to be associated with deep gas migration channels[52]. Furthermore, across the East Greenland shelf, $\delta^{13}C$ records in benthic and planktonic foraminifera indicate at least three methane release episodes since deglaciation related to dissociating hydrates[53]. It is also likely that many GHPs that reside outside of the present-day GHSZ have collapsed, forming large depressions – a phenomenon that has been widely reported in previously glaciated trough systems in the Arctic[13,14,54].

Despite considerable seafloor methane seepage from formerly glaciated Arctic shelves, the actual flux of methane that attains the atmosphere remains unconstrained. Recent studies show that a broad gas-seepage area extending along the North-Western Barents sea from 74° to 79° contributed only 0.07% to net atmospheric methane[3]. This finding resonates with recent airborne measurements revealing a distinct absence of high atmospheric methane concentration during the summer[55]. The role of the water column in critically regulating methane transfer to the atmosphere is not fully understood, and it remains unclear as to whether oceanic methane degradation has limits where large and abrupt fluxes of seafloor release could overcome filter systems thereby forcing a potent atmospheric feedback as has previously been proposed.

The earth has experienced a wide range of climate extremes over its geological history[56] such as the Permian-Triassic catastrophe 252 Mio years ago[57] when both carbon-dioxide and methane were released on a massive scale into the atmosphere. It has recently been proposed that such an event was reinforced by global-scale hydrate dissociation and methane release triggered by initial global warming after a prolonged "snow-ball earth" glacial episode[58]. Our inferences regarding a glacial gas hydrate capacitor are worth consideration when investigating the causes of past episodes of global-scale gas methane release evident in the geological record.

Despite the growing number of seep-related features that have been recently discovered across the seafloor of the Arctic, shallow gas hydrate systems remain poorly understood and documented, particularly where they have undergone a complex environmental history. This study reveals that abrupt changes in pressure and temperature conditions associated with the interplay of grounded ice, post-glacial isostatic rebound and influx of variable ocean currents all critically modulate the gas hydrate stability zone thereby driving distinct episodes of natural gas storage and release. To date, these processes have not been well described or quantified, and any attempt to understand the past and determine the future impact of Arctic methane emissions on global climate need to comprehensively account for them.

Methods

Description of methods of seismic and hydroacoustic data acquisition and processing, sediment sampling and geochemical analyses provided in SI Methods. SI Methods also contains extensive description of ice-sheet model and conductive heat flux model of gas hydrate stability zone.

Acknowledgements

The research is part of the centre for Arctic Gas Hydrate, Environment and Climate and was supported by the Research Council of Norway through its Centres of Excellence funding scheme grant No. 223259. We thank the crew of the RV *Helmer Hanssen* for their assistance in sediment and water sampling and acquisition of the seismic data. We are also thankful to Kate Waghorn for processing 2D seismic lines.

1 Shakhova, N. *et al.* The East Siberian Arctic Shelf: towards further assessment of permafrost-related methane fluxes and role of sea ice. *Philosophical Transactions of the Royal Society of London A: Mathematical, Physical and Engineering Sciences* **373**, doi:10.1098/rsta.2014.0451 (2015).

2 Paull, C. K. *et al.* Active mud volcanoes on the continental slope of the Canadian Beaufort Sea. *Geochemistry, Geophysics, Geosystems* **16**, 3160-3181, doi:10.1002/2015GC005928 (2015).

3 Mau, S. *et al.* Widespread methane seepage along the continental margin off Svalbard - from Bjørnøya to Kongsfjorden. *Scientific Reports* **7**, 42997, doi:10.1038/srep42997 http://www.nature.com/articles/srep42997#supplementary-information (2017).

4 Sloan, E. D. & Koh, C. A. *Clathrate Hydrates of Natural Gases, Third Edition*. (CRC Press, 2008).

5 Dickens, G. R. Rethinking the global carbon cycle with a large, dynamic and microbially mediated gas hydrate capacitor. *Earth and Planetary Science Letters* **213**, 169-183, doi:http://dx.doi.org/10.1016/S0012-821X(03)00325-X (2003).

6 Shakhova, N. *et al.* Ebullition and storm-induced methane release from the East Siberian Arctic Shelf. *Nature Geosci* **7**, 64-70, doi:10.1038/ngeo2007 http://www.nature.com/ngeo/journal/v7/n1/abs/ngeo2007.html#supplementary-information (2014).

7 Thomas, D. J., Zachos, J. C., Bralower, T. J., Thomas, E. & Bohaty, S. Warming the fuel for the fire: Evidence for the thermal dissociation of methane hydrate during the Paleocene-Eocene thermal maximum. *Geology* **30**, 1067-1070, doi:10.1130/0091-7613(2002)030<1067:wtfftf>2.0.co;2 (2002).

8 Reeburgh, W. S. Oceanic Methane Biogeochemistry. *Chemical Reviews* **107**, 486-513, doi:10.1021/cr050362v (2007).

9 Bernardino, A. F., Levin, L. A., Thurber, A. R. & Smith, C. R. Comparative Composition, Diversity and Trophic Ecology of Sediment Macrofauna at Vents, Seeps and Organic Falls. *PLoS ONE* **7**, e33515, doi:10.1371/journal.pone.0033515 (2012).

10 Åström, E. K. L., Carroll, M. L., Ambrose, W. G., Jr. & Carroll, J. Arctic cold seeps in marine methane hydrate environments: impacts on shelf macrobenthic community structure offshore Svalbard. *Marine Ecology Progress Series* **552**, 1-18 (2016).

11 Pop Ristova, P., Wenzhofer, F., Ramette, A., Felden, J. & Boetius, A. Spatial scales of bacterial

community diversity at cold seeps (Eastern Mediterranean Sea). *ISME J* **9**, 1306-1318, doi:10.1038/ismej.2014.217 (2015).
12 Mienert, J. in *Encyclopedia of Ocean Sciences (Second Edition)* 790-798 (Academic Press, 2009).
13 Portnov, A., Vadakkepuliyambatta, S., Mienert, J. & Hubbard, A. Ice-sheet-driven methane storage and release in the Arctic. *Nat Commun* **7**, doi:10.1038/ncomms10314 (2016).
14 Long, D., Lammers, S. & Linke, P. Possible hydrate mounds within large sea-floor craters in the Barents Sea. *Geological Society, London, Special Publications* **137**, 223-237, doi:10.1144/gsl.sp.1998.137.01.18 (1998).
15 Koch, S. *et al.* Gas-controlled seafloor doming. *Geology* **43**, 571-574, doi:10.1130/g36596.1 (2015).
16 Ruppel, C. Tapping Methane Hydrates for Unconventional Natural Gas. *Elements* **3**, 193-199, doi:10.2113/gselements.3.3.193 (2007).
17 Westbrook, G. K. *et al.* Escape of methane gas from the seabed along the West Spitsbergen continental margin. *Geophysical Research Letters* **36**, n/a-n/a, doi:10.1029/2009GL039191 (2009).
18 Ferré, B., Mienert, J. & Feseker, T. Ocean temperature variability for the past 60 years on the Norwegian-Svalbard margin influences gas hydrate stability on human time scales. *Journal of Geophysical Research: Oceans* **117**, n/a-n/a, doi:10.1029/2012JC008300 (2012).
19 Berndt, C. *et al.* Temporal Constraints on Hydrate-Controlled Methane Seepage off Svalbard. *Science* **343**, 284-287, doi:10.1126/science.1246298 (2014).
20 Mackay, J. R. Pingo Growth and collapse, Tuktoyaktuk Peninsula Area, Western Arctic Coast, Canada: a long-term field study. *Géographie physique et Quaternaire* **52**, 271-323, doi:10.7202/004847ar (1998).
21 Paull, C. K. *et al.* Origin of pingo-like features on the Beaufort Sea shelf and their possible relationship to decomposing methane gas hydrates. *Geophysical Research Letters* **34**, n/a-n/a, doi:10.1029/2006GL027977 (2007).
22 Serov, P., Portnov, A., Mienert, J., Semenov, P. & Ilatovskaya, P. Methane release from pingo-like features across the South Kara Sea shelf, an area of thawing offshore permafrost. *Journal of Geophysical Research: Earth Surface* **120**, 1515-1529, doi:10.1002/2015JF003467 (2015).
23 Shearer, J. M., Macnab, R. F., Pelletier, B. R. & Smith, T. B. Submarine pingos in the beaufort sea. *Science* **174**, 816-818, doi:10.1126/science.174.4011.816 (1971).
24 Auriac, A. *et al.* Glacial isostatic adjustment associated with the Barents Sea ice sheet: A modelling inter-comparison. *Quaternary Science Reviews* **147**, 122-135, doi:http://dx.doi.org/10.1016/j.quascirev.2016.02.011 (2016).
25 Patton, H. & Andreassen, K., Winsborrow, M.C.M., Stroeven, A., Hubbard, A. The build-up, configuration, and dynamical sensitivity of the Eurasian ice-sheet complex to Late Weichselian climate and ocean forcing. *Quaternary Science Reviews* (2016).
26 Patton, H. *et al.* Geophysical constraints on the dynamics and retreat of the Barents Sea ice sheet as a paleobenchmark for models of marine ice sheet deglaciation. *Reviews of Geophysics* **53**, 1051-1098, doi:10.1002/2015RG000495 (2015).
27 Jessen, S. P., Rasmussen, T. L., Nielsen, T. & Solheim, A. A new Late Weichselian and Holocene marine chronology for the western Svalbard slope 30,000–0 cal years BP. *Quaternary Science Reviews* **29**, 1301-1312, doi:http://dx.doi.org/10.1016/j.quascirev.2010.02.020 (2010).
28 Rasmussen, T. L. & Thomsen, E. Palaeoceanographic development in Storfjorden, Svalbard, during the deglaciation and Holocene: evidence from benthic foraminiferal records. *Boreas* **44**, 24-44, doi:10.1111/bor.12098 (2015).
29 Lucchi, R. G. *et al.* Postglacial sedimentary processes on the Storfjorden and Kveithola trough mouth fans: Significance of extreme glacimarine sedimentation. *Global and Planetary Change* **111**, 309-326, doi:http://dx.doi.org/10.1016/j.gloplacha.2013.10.008 (2013).
30 Rasmussen, T. L. *et al.* Paleoceanographic evolution of the SW Svalbard margin (76°N) since 20,000 14C yr BP. *Quaternary Research* **67**, 100-114, doi:http://dx.doi.org/10.1016/j.yqres.2006.07.002 (2007).
31 M. Ł ¸acka, M. Z. a., M. Forwick, and W. Szczucinski. Late Weichselian and Holocene palaeoceanography of Storfjordrenna, southern Svalbard. *Climate of the past* **11**, 587-603, doi:doi:10.5194/cp-11-587-2015 (2015).
32 McGinnis, D. F., Greinert, J., Artemov, Y., Beaubien, S. E. & Wüest, A. Fate of rising methane bubbles in stratified waters: How much methane reaches the atmosphere? *Journal of Geophysical Research: Oceans* **111**, n/a-n/a, doi:10.1029/2005JC003183 (2006).
33 Greinert, J., Artemov, Y., Egorov, V., De Batist, M. & McGinnis, D. 1300-m-high rising bubbles from mud volcanoes at 2080 m in the Black Sea: Hydroacoustic characteristics and temporal variability. *Earth and Planetary Science Letters* **244**, 1-15, doi:http://dx.doi.org/10.1016/j.epsl.2006.02.011 (2006).
34 Greinert, J. Monitoring temporal variability of bubble release at seeps: The hydroacoustic swath system GasQuant. *Journal of Geophysical Research: Oceans* **113**, n/a-n/a, doi:10.1029/2007JC004704 (2008).
35 Piñero, E. *et al.* Gas hydrate disturbance fabrics of southern Hydrate Ridge sediments (ODP Leg 204): Relationship with texture and physical properties. *Geo-Marine Letters* **27**, 279-288, doi:10.1007/s00367-007-0077-z (2007).
36 Waite, W. F., Kneafsey, T. J., Winters, W. J. & Mason, D. H. Physical property changes in hydrate-bearing sediment due to depressurization and subsequent repressurization. *Journal of Geophysical Research: Solid Earth* **113**, n/a-n/a, doi:10.1029/2007JB005351 (2008).
37 Bergh, S. G. & Grogan, P. Tertiary structure of the Sørkapp-Hornsund Region, South Spitsbergen, and implications for the offshore southern extension of the fold-thrust Belt. *Norwegian Journal of Geology* **83**, 43-60 (2003).
38 GROGAN, P. *et al.* Structural elements and petroleum geology of the Norwegian sector of the northern Barents Sea. *Geological Society, London, Petroleum Geology Conference series* **5**, 247-259, doi:10.1144/0050247 (1999).
39 Chatterjee, S. *et al.* The impact of lithologic heterogeneity and focused fluid flow upon gas hydrate distribution in marine sediments. *Journal of Geophysical Research: Solid Earth* **119**, 6705-6732, doi:10.1002/2014JB011236 (2014).
40 Ingólfsson, Ó. & Landvik, J. Y. The Svalbard–Barents Sea ice-sheet – Historical, current and future perspectives. *Quaternary Science Reviews* **64**, 33-60, doi:http://dx.doi.org/10.1016/j.quascirev.2012.11.034 (2013).
41 Walczowski, W. Frontal structures in the West Spitsbergen Current margins. *Ocean Sci.* **9**, 957-975, doi:10.5194/os-9-957-2013 (2013).
42 Boyer, T. P., J. I. Antonov, O. K. Baranova, C. Coleman, H. E. Garcia, A. Grodsky, D. R. Johnson, R. A. Locarnini, A. V. Mishonov, T.D. O'Brien, C.R. Paver, J.R. Reagan, D. Seidov, I. V. Smolyar, and M. M. Zweng. *World Ocean Database 2013*. Vol. 72 (Silver Spring, 2013).
43 Bohrmann, G., Greinert, J., Suess, E. & Torres, M. Authigenic carbonates from the Cascadia subduction zone and their relation to gas hydrate stability. *Geology* **26**, 647-650, doi:10.1130/0091-7613(1998)026<0647:acftcs>2.3.co;2 (1998).
44 Hovland, M., Talbot, M. R., Qvale, H., Olaussen, S. & Aasberg, L. Methane-related carbonate cements in pockmarks of the North Sea. *Journal of Sedimentary Research* **57**, 881-892, doi:10.1306/212f8c92-2b24-11d7-8648000102c1865d (1987).
45 Koch, S. *et al.* Gas-controlled seafloor doming. *Geology*, doi:10.1130/g36596.1 (2015).
46 Barry, M. A., Boudreau, B. P. & Johnson, B. D. Gas domes in soft cohesive sediments. *Geology* **40**, 379-382, doi:10.1130/g32686.1 (2012).
47 Cremiere, A. *et al.* Timescales of methane seepage on the Norwegian margin following collapse of the Scandinavian Ice Sheet. *Nat Commun* **7**, doi:10.1038/ncomms11509 (2016).
48 Pecher, I. A., Henrys, S. A., Ellis, S., Chiswell, S. M. & Kukowski, N. Erosion of the seafloor at the top of the gas hydrate stability zone on the Hikurangi Margin, New Zealand. *Geophysical Research Letters* **32**, n/a-n/a, doi:10.1029/2005GL024687 (2005).
49 Knies, J., Vogt, C. & Stein, R. Late Quaternary growth and decay of the Svalbard/Barents Sea ice sheet and paleoceanographic evolution in the adjacent Arctic Ocean. *Geo-Marine Letters* **18**, 195-202, doi:10.1007/s003670050068 (1998).
50 Hald, M. *et al.* Late-glacial and Holocene paleoceanography and sedimentary environments in the St. Anna Trough, Eurasian Arctic Ocean margin. *Palaeogeography, Palaeoclimatology, Palaeoecology* **146**, 229-249, doi:http://dx.doi.org/10.1016/S0031-0182(98)00133-3 (1999).
51 Moros, M., Jensen, K. G. & Kuijpers, A. Mid-to late-Holocene hydrological and climatic variability in Disko Bugt, central West Greenland. *The Holocene* **16**, 357-367, doi:10.1191/0959683606hl933rp (2006).
52 Nielsen, T. *et al.* Fluid flow and methane occurrences in the Disko Bugt area offshore West Greenland: indications for gas hydrates? *Geo-Marine Letters* **34**, 511-523, doi:10.1007/s00367-014-0382-2 (2014).
53 Smith, L. M., Sachs, J. P., Jennings, A. E., Anderson, D. M. & deVernal, A. Light δ13C events during deglaciation of the East Greenland Continental Shelf attributed to methane release from gas hydrates. *Geophysical Research Letters* **28**, 2217-2220, doi:10.1029/2000GL012627 (2001).
54 Roy, S., Hovland, M., Noormets, R. & Olaussen, S. Seepage in Isfjorden and its tributary fjords, West Spitsbergen. *Marine Geology* **363**, 146-159, doi:http://dx.doi.org/10.1016/j.margeo.2015.02.003 (2015).
55 Myhre, C. L. *et al.* Extensive release of methane from Arctic seabed west of Svalbard during summer 2014 does not influence the atmosphere. *Geophysical Research Letters* **43**, 4624-4631, doi:10.1002/2016GL068999 (2016).
56 Snyder, C. W. Evolution of global temperature over the past two million years. *Nature* **538**, 226-228, doi:10.1038/nature19798 http://www.nature.com/nature/journal/v538/n7624/abs/nature19798.html#supplementary-information (2016).
57 Brand, U. *et al.* Methane Hydrate: Killer cause of Earth's greatest mass extinction. *Palaeoworld* **25**, 496-507, doi:http://doi.org/10.1016/j.palwor.2016.06.002 (2016).
58 Hyde, W. T., Crowley, T. J., Baum, S. K. & Peltier, W. R. Neoproterozoic /`snowball Earth/' simulations with a coupled climate/ice-sheet model. *Nature* **405**, 425-429 (2000).
59 Waelbroeck, C. *et al.* Sea-level and deep water temperature changes derived from benthic foraminifera isotopic records. *Quaternary Science Reviews* **21**, 295-305, doi:http://dx.doi.org/10.1016/S0277-3791(01)00101-9 (2002).